Vibron-assisted spin relaxation at a metal/organic interface

A. Droghetti,[1,*] I. Rungger,[1,†] M. Cinchetti,[2] and S. Sanvito[1]

[1]*School of Physics, AMBER and CRANN Institute, Trinity College, Dublin 2, Ireland*

[2]*Department of Physics and Research Center OPTIMAS, University of Kaiserslautern, Erwin-Schrödinger Straße 46, 67663 Kaiserslautern, Germany*

(Received 28 January 2015; revised manuscript received 4 June 2015; published 24 June 2015)

Inspired by recent experiments for hybrid organic-ferromagnet interfaces, we propose a spin-relaxation mechanism which does not depend on either the spin-orbit or the hyperfine interaction. This takes place when a molecule with initial spin imbalance is weakly coupled to a metal surface and can be excited in various vibrational states. In such a situation the electron-vibron interaction promotes the exchange of spin-polarized electrons between the molecule and the surface, serving as an energy and angular momentum reservoir. This process leads to an effective spin relaxation of the electron population in the molecule. We suggest that this nonequilibrium mechanism can be investigated through time-resolved spin-polarized scanning tunneling microscopy experiments.

DOI: 10.1103/PhysRevB.91.224427 PACS number(s): 72.25.Mk, 72.25.Rb, 73.23.Hk

I. INTRODUCTION

Organic spintronics [1,2] is the study of spin-dependent electronic transport in organic semiconductors. These materials have potential for novel device applications owing to their long spin lifetimes [3,4], but at present there is an open debate about the causes of spin relaxation [5–7], with the hyperfine interaction associated with hydrogen [8–10] and the spin-orbit coupling [11–14] being the two suggested mechanisms. Besides the study of spin transport in bulk organic materials, significant research effort has been dedicated to understand the electronic properties of hybrid interfaces between molecules and ferromagnetic metals, and their relation to the spin-injection process [15,16]. However, so far, most of the work has focused on measuring the energy level alignment [17–21] and the interface states [19–26], while very few studies have addressed the fast spin dynamics.

In an important work, Steil *et al.* [27] measured the spin lifetime of a state at the interface between tris(8-hydroxyquinolinato)-aluminum(III) (Alq_3) and Co by two-photon photoemission (2PPE). The experiment showed that the majority spins relax twice as fast as the minority, with typical lifetimes of the order of picoseconds. Remarkably, these results are in contrast to those usually reported for free ferromagnetic surfaces, where the spin relaxation time is several orders of magnitude shorter and the minority excited electrons decay faster than the majority [28]. This indicates that spin relaxation at hybrid interfaces is a complex phenomenon that challenges our fundamental understanding. Furthermore, it may have dramatic consequences for the operation of devices, since spin relaxation may occur already in the first few molecular layers near the electrode, regardless of the intrinsic properties of the organic compound and of the bulk spin relaxation.

In this article we propose a mechanism which accounts for spin relaxation at hybrid interfaces and does not involve either spin-orbit coupling or hyperfine interaction in the molecules. This mechanism is the result of a series of allowed charge and spin exchange processes between the molecules and the substrate, whose rates depend on the interaction of electrons with the molecular vibrations. Such processes have the net effect of changing the relative occupation of the two spin directions in the organic, thus leading to a net spin depolarization. Hereby the metal surface serves as a reservoir for energy and angular momentum, and no spin relaxation occurs in the molecule in the absence of electron-vibron interaction. Although this mechanism may be partly responsible for the spin-dependent lifetime reported in the experiments by Steil *et al.* [27], a quantitative analysis is rather difficult. In fact, in actual samples, an amorphous Alq_3 thin layer is deposited on Co resulting in a large spread of the molecule-substrate couplings and in a ill-defined interface. Therefore, here we suggest an alternative direct way to measure the proposed spin-relaxation mechanism. This consists in performing time-resolved spin-polarized scanning tunneling microscopy (spSTM) experiments which probe well-defined molecules on a substrate. We will show that the required time resolution is indeed achievable with this technique [29–32]. The article is organized as follows: First, we introduce the proposed model and we describe the employed theoretical methods (Sec. II). Then we present the results, discuss their physical interpretation, and analyze their dependence on the model parameters (Sec. III). Finally, before concluding, we show some transport simulations which demonstrate that the proposed spin-relaxation effect could be measured in spSTM experiments (Sec. IV).

II. MODEL AND METHOD

We model the molecule by means of a single molecular energy level ϵ_d and a single vibrational mode of frequency ω (see Fig. 1). This choice is supported by the fact that often only the mode with the largest coupling to the electrons is relevant for transport experiments at the molecular scale [33]. The molecule is assumed weakly coupled to an electrode, which acts as a charge reservoir at the chemical potential $\mu = 0$. The total (molecule plus electrode) Hamiltonian reads [34–38] $H = H_{\rm mol} + H_{\rm lead} + H_{\rm t}$. The Hamiltonian of the

*Present address: Nano-Bio Spectroscopy Group and European Theoretical Spectroscopy Facility (ETSF), Universidad del Pais Vasco CFM CSIC-UPV/EHU-MPC and DIPC, Av. Tolosa 72, 20018 San Sebastian, Spain.

†Present address: National Physical Laboratory, Hampton Road, TW11 OLW, United Kingdom.

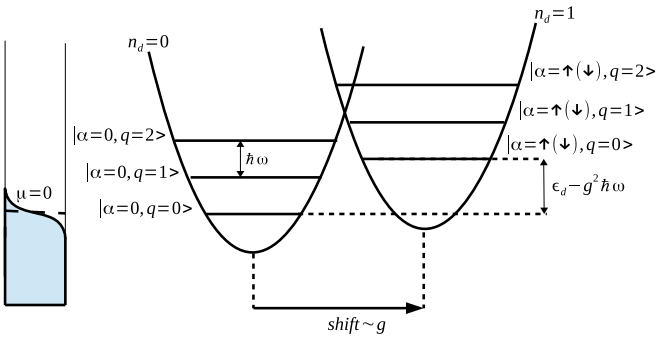

FIG. 1. (Color online) Cartoon describing the system. A metal surface (left), represented by its Fermi distribution with chemical potential μ, can exchange charges with a molecule, described by a Franck-Condon diagram (right). The potential energy surfaces for the molecule in the $n_d = 0$ and $n_d = 1$ charging states are shifted with respect to each other by g. For a given charging state we show the three lowest energy levels and the electron injection energy barrier $E_{\alpha=\uparrow(\downarrow),q=0} - E_{\alpha=0,q=0} = (\epsilon_d - g^2\hbar\omega) \equiv \tilde{\epsilon}_d$.

electrode $H_{\rm lead}$, and the coupling Hamiltonian $H_{\rm t}$, have standard forms, and we refer to Refs. [34–38] for details. $H_{\rm t}$ is proportional to a tunneling amplitude V between the molecule and the electrode. Weak coupling means that any relevant energy difference in the problem is much larger than V. The Hamiltonian of the molecule reads

$$H_{\rm mol} = \epsilon_d \hat{n}_d + \frac{U}{2}\hat{n}_d(\hat{n}_d - 1) + g\hbar\omega(b^\dagger + b)\hat{n}_d + \hbar\omega\left(b^\dagger b + \frac{1}{2}\right). \quad (1)$$

The operator $d_\sigma^\dagger$ (d_σ) creates (annihilates) an electron of spin σ on the molecule ($\hat{n}_d = \sum_\sigma d_\sigma^\dagger d_\sigma$), and $b^\dagger$ (b) creates (annihilates) a vibron. The molecule charging energy is U. The term $g\hbar\omega(b^\dagger + b)\hat{n}_d$ in $H_{\rm mol}$ describes an electron-vibron coupling with coupling constant g.

$H_{\rm mol}$ is diagonalized by the Lang-Firsov canonical transformation [36,37,39,40], and the eigenenergies are

$$E_{\alpha q} = \tilde{\epsilon}_d n_{d,\alpha} + \frac{\tilde{U}}{2} n_{d,\alpha}(n_{d,\alpha} - 1) + \hbar\omega\left(q + \frac{1}{2}\right), \quad (2)$$

with $\tilde{\epsilon}_d \equiv \epsilon_d - g^2\hbar\omega$ and $\tilde{U} \equiv (U - 2g^2\hbar\omega)$ being the renormalized molecular and charging energies, respectively. The corresponding eigenstates are $|\alpha,q\rangle$, where $\alpha \in \{0,\uparrow,\downarrow,\uparrow\downarrow\}$ specifies the electronic state, $q = \{0,1,2,3,\dots\}$ is the vibron occupation number, and $n_{d,\alpha} = \{0,1,2\}$ is the number of electrons in $|\alpha,q\rangle$, i.e., $\hat{n}_d|\alpha,q\rangle = n_{d,\alpha}|\alpha,q\rangle$ [41].

The energy difference $E_{\uparrow(\downarrow),0} - E_{0,0} = \tilde{\epsilon}_d$ between $|\alpha = \uparrow(\downarrow),q = 0\rangle$ and $|\alpha = 0,q = 0\rangle$ can be interpreted as the electron injection energy barrier (see Fig. 1).

We treat tunneling as a perturbation and evaluate the dynamics of our system through a master equation [38,40]

$$\dot{P}_{\alpha q}(t) = \sum_{\alpha' q'} \Lambda_{\alpha' q',\alpha q} P_{\alpha' q'}(t), \quad (3)$$

where $\Lambda_{\alpha' q',\alpha q} = R_{\alpha' q' \to \alpha q} - \delta_{\alpha' q',\alpha q} \sum_{\alpha'' q''} R_{\alpha' q' \to \alpha'' q''}$. This describes the time evolution of the probabilities $P_{\alpha q}$ of occupying a state with quantum numbers $\{\alpha,q\}$ through a

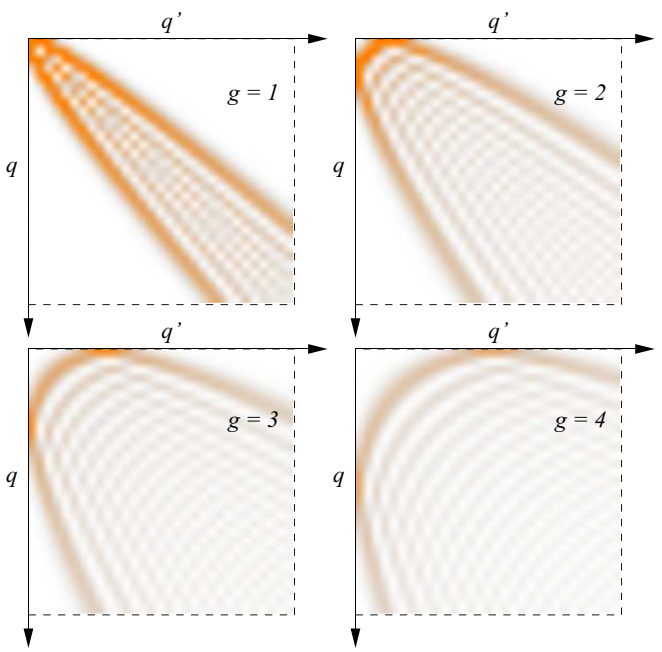

FIG. 2. (Color online) Squared values of the FC matrix elements $|F_{qq'}|^2$ for $0 \leqslant q,q' \leqslant 30$ and for $g = 1,2,3,4$.

Markov process [42]. The transition rates are

$$R_{\alpha q \to \alpha' q'} = \sum_\sigma \frac{\Gamma_{s,\sigma}}{\hbar} f(E_{\alpha' q'} - E_{\alpha q}) \times \left(\left|D^\sigma_{\alpha\alpha'}\right|^2 |F_{qq'}|^2 + \left|D^\sigma_{\alpha'\alpha}\right|^2 |F_{q'q}|^2\right), \quad (4)$$

where f is the Fermi function and $\Gamma_{s,\sigma} = 2\pi V \rho_\sigma$ is the effective electrode-molecule coupling, which depends on electrode density of states ρ_σ. $D^\sigma_{\alpha\alpha'} = \langle\alpha|d_\sigma|\alpha'\rangle$ are the electronic matrix elements, while $F_{qq'}$ are the Franck-Condon (FC) matrix elements between two states with q and q' vibrons [35,37,38], which read

$$F_{qq'} = \sqrt{\frac{q_<!}{q_>!}} g^{q_> - q_<} e^{-\frac{g^2}{2}} L^{q_> - q_<}_{q_<}(g^2) \begin{cases} (-1)^{q-q'} & \text{if } q \geqslant q', \\ 1 & \text{if } q < q', \end{cases} \quad (5)$$

where g is the electron-vibron coupling, $q_> = \max(q,q')$, and $L^i_j(x)$ are the generalized Laguerre polynomials. The squared values of the FC matrix elements $|F_{qq'}|^2$ are plotted in Fig. 2 for $g = 1,2,3,4$. For small g the FC matrix is almost diagonal, while for large g, transitions between low lying vibron states are suppressed.

The general solution [43] of Eq. (3) is

$$P_{\alpha q}(t) = \sum_i c_i \xi^i_{\alpha q} e^{-t/\tau_i}, \quad (6)$$

where $-1/\tau_i = \lambda_i$ and $\{\xi^i_{\alpha q}\}$ are, respectively, the ith eigenvalue and eigenvector of the matrix Λ. The constants c_i are determined by the initial condition $P_{\alpha q}(0)$. Although Λ is not Hermitian, all λ_i are real and negative ($\tau_i > 0$), except for λ_1, which vanishes ($\tau_1 = \infty$) [43]. The expression for $P_{\alpha q}(t)$, therefore, is a sum of many decaying exponents, each one characterized by the relaxation time τ_i. The existence of $\lambda_1 = 0$

implies that in the infinite time limit a stationary solution is always reached, and the probability of being in a state with quantum numbers α and q is $c_1\xi^1_{\alpha q}$.

III. RESULTS

In order to evaluate the spin-relaxation time we choose an initial condition with a significant spin imbalance, which can be obtained experimentally for instance via optical excitation from the spin-splitted d band of the magnetic electrode [27,44], or else by application of a large magnetic field, switched off at time 0. Then we evaluate the time evolution of the probabilities $\{P_{\alpha q}(t)\}$ computed by solving Eq. (3), with initial conditions $P_{\uparrow,0}(0) = 0.8$, $P_{\downarrow,0}(0) = 0.2$, and $P_{\alpha q}(0) = 0$ for any other pair $\{\alpha,q\}$ [45]. We set $\Gamma = \Gamma_{s,\uparrow} = \Gamma_{s,\downarrow}$ to be constant, which means that the molecular state is hybridized only with the largely energy independent and spin degenerate s band of the transition metal. This extends much further away from the surface than the spin-split d bands. Note that we assume the molecule to be weakly coupled to the surface, so that the formation of spin-split hybrid states can be neglected. Although we chose a rather large value for $|P^{n=\uparrow,q=0}(0) - P^{n=\downarrow,q=0}(0)|$ in order to magnify the effect, we have verified that the results are qualitatively independent of the initial spin population as long as $P_{\uparrow,0}(0) > P_{\downarrow,0}(0)$. Furthermore, they hold also assuming a small nonzero initial probability for states with $\alpha = \uparrow(\downarrow)$ and $q \neq 0$. In a similar way, the study can be extended to the case when $\Gamma_\uparrow \neq \Gamma_\downarrow$. Throughout this work, the renormalized charging energy is set to $\tilde{U} = 4$ so to be repulsive and disfavoring the double occupation of the molecule and $\tilde{\epsilon}_d$ is kept positive so that the ground state of $H_{\rm mol}$ is $|\alpha = 0,q = 0\rangle$, i.e., the level is empty and with no vibrons (note that $\tilde{\epsilon}_d$, $\tilde{U}$ and the temperature $k_{\rm B}T$ are in units of $\hbar\omega$).

As representative results in Fig. 3 we show $\{P_{\alpha q}(t)\}$, for $\tilde{\epsilon}_d = 4$, $g = 0,2,4$, and $k_{\rm B}T = 0.2$. When $g = 0$, i.e., there is no electron-vibron coupling, $P_{\uparrow(\downarrow),0}$ decays exponentially in time, with the decay constant simply determined by the coupling to the electrode. At the same time $P_{0,0}(t)$ increases with time up to $P_{0,0}(t) = 1$, when the system reaches its ground state. Importantly, the average number of electrons N_e and the spin polarization of the molecule S^z also decay exponentially with the same constant (upper right panel of Fig. 3). This means that the relative spin-polarization $S_P = S^z/N_e$ is constant in time and there is no net spin relaxation as expected for a model which does not include explicitly any spin-flip term, such as spin orbit. Note that in this case, for the chosen initial conditions, no vibrons are excited since the FC matrix, whose elements $F_{qq'}$ enter the transition rates of Eq. (4), is the identity matrix [35,37,38].

In contrast, when electrons on the molecule couple to the vibron ($g \neq 0$), the decay of N_e and S^z becomes progressively slower as g increases (note the different time scales in the graphs of Fig. 3) and S_P is surprisingly no longer constant in time. In fact for strong enough coupling (e.g., $g = 4$), S_P vanishes when N_e is still large, i.e., the spin on the molecule relaxes. The picture is then that of electrons being on average trapped on the molecule for long times, during which their spin population becomes fully depolarized. This vibron-induced mechanism for spin relaxation represents the main finding of our work.

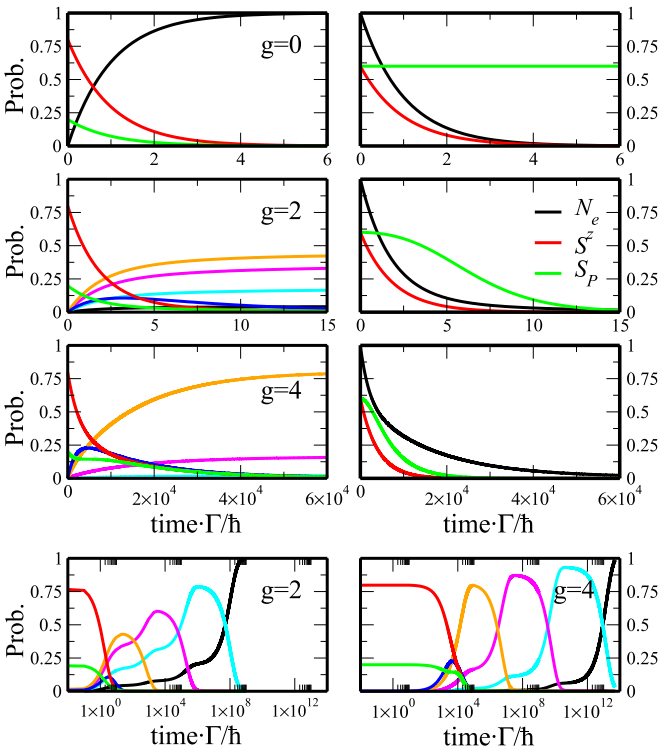

FIG. 3. (Color online) Time evolution of the occupation probabilities $\{P_{\alpha,q}\}$ (left panels) and of the average number of electrons N_e, spin polarization S^z, and relative spin polarization $S_{\rm P}$ (right panels) for $g = 0,2,4$ ($k_{\rm B}T = 0.2$). Here $\tilde{\epsilon}_d = 4$ and $\tilde{U} = 4$. The results are for $P_{0,0}$ (black), $P_{0,1}$ (cyan), $P_{0,2}$ (magenta), $P_{0,3}$ (orange), $P_{0,4}$ (blue), $P_{\uparrow,0}$ (red), and $P_{\downarrow,0}$ (green), while here $P_{\alpha,q} \approx 0$ for $q > 4$. The two lower panels display $\{P_{\alpha,q}\}$ for $g = 2$ and $g = 4$, but plotted on a log scale over a long time interval.

In order to understand such behavior, we inspect the time evolution of the individual $P_{\alpha,q}(t)$. We see in Fig. 3 that the decay rates become systematically slower for larger g and several states with no electrons, but containing several vibrons, acquire a finite probability of being populated during the transient regime. These are long living and die out over a much longer time scale, eventually bringing the system to its ground state $|\alpha = 0,q = 0\rangle$ (see lower panels of Fig. 3). The inclusion in the model of vibron dissipation can result in a faster relaxation, but the overall results remain valid as long as the vibron dissipation rate is small compared to the electron one.

This evolution follows from the important fact that now the FC matrix is nondiagonal and transitions from $|\alpha = \uparrow(\downarrow),q = 0\rangle$ to some of the states $|\alpha = 0,q \neq 0\rangle$ become allowed [35,37,38]. For a small g (e.g., $g = 1$), the transition rates from $|\alpha = \uparrow(\downarrow),q = 0\rangle$ to the states $|\alpha = 0,q = n\rangle$ ($n = 1, 2, 3$) are the largest, while all the others are negligible. These transitions correspond to the process schematically sketched in Fig. 4(a), where an electron is transferred to the surface leaving the molecule empty in a state of lower energy, but vibrationally excited. For a large g, the same transitions become less probable, since the corresponding FC matrix elements are negligible. In fact, the matrix elements connecting $|\alpha = \uparrow(\downarrow),q = 0\rangle$ to $|\alpha = 0,q \geqslant 5\rangle$ are the largest, but the related transitions are energetically not allowed, i.e.,

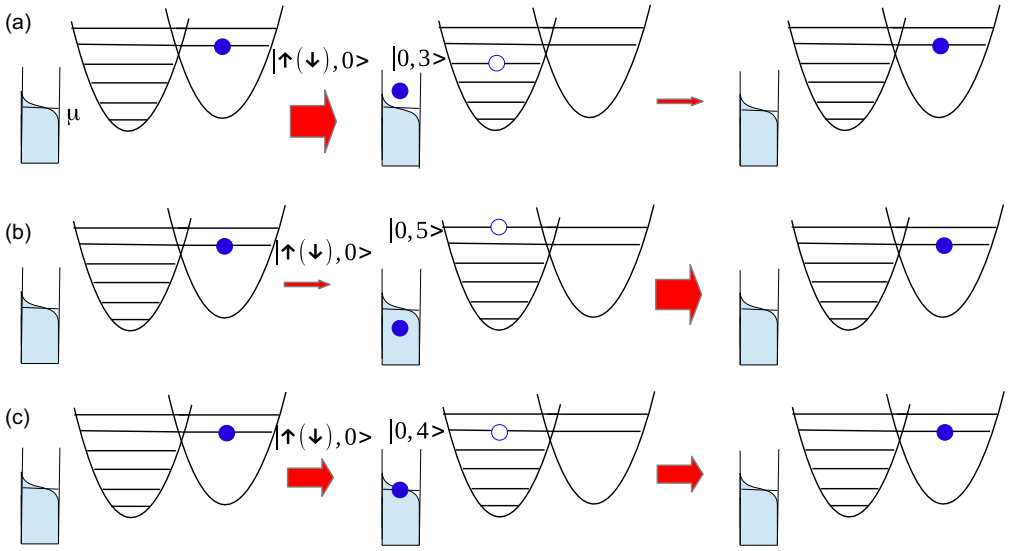

FIG. 4. (Color online) Cartoon illustrating possible transitions, with the arrows' size indicating the relative rates. An electron (blue sphere) is transferred to the surface, leaving the molecule in a state with no electron of (a) lower energy, the opposite process is suppressed since it is unlikely to find an electron at high energies above μ in the metal; (b) higher energy, the process itself has low probability since it is unlikely to find an empty state in the metal far below μ; and (c) approximately the same energy, the opposite process has a similar probability. Only process (c) leads to significant electron exchange both from surface to molecule and vice versa. Since the initial and final spin on the molecule are not related, the process can lead to an effective spin relaxation on the molecule.

$E_{\uparrow(\downarrow),0} - E_{0,q\geqslant 5} \gg k_B T$. This means that the system will be blocked in the initial state for a longer time, as demonstrated by the monotonic increase of the lifetime of $|\alpha = \uparrow(\downarrow), q = 0\rangle$ with g (Fig. 3). This is in essence a manifestation of the FC blockade predicted for molecular transistors [36,37] and recently observed experimentally [46].

Next, in order to understand the behavior of S_P, we observe from Fig. 3 that for $g = \{2,4\}$, as soon as the probability $P_{0,4}(t)$ for $|\alpha = 0, q = 4\rangle$ reaches a maximum, $P_{\downarrow,0}(t)$ changes its characteristic decay. This becomes much slower until the characteristic time t', when $P_{\downarrow,0}(t') = P_{\uparrow,0}(t') \neq 0$. Then both $P_{\downarrow,0}(t)$ and $P_{\uparrow,0}(t)$ start to relax at the same rate. This occurs because the states $|\alpha = \uparrow(\downarrow), q = 0\rangle$ are resonant with $|\alpha = 0, q = 4\rangle$, i.e., $E_{\uparrow(\downarrow),0} = E_{0,4}$ [see Fig. 4(c)]. Then the transition rates $R_{\alpha,0\to 0,4}$ and $R_{0,4\to\alpha,0}$ ($\alpha = \uparrow,\downarrow$) are equal, and during the transient time, the relaxation process balances the three probabilities $P_{\alpha,0}(t)$ ($\alpha = \uparrow,\downarrow$) and $P_{0,4}(t)$. Since $H_{\rm mol}$ does not contain any term explicitly breaking the spin degeneracy, the system tends to dynamically equilibrate the spin dependent electron occupation probabilities.

We expect the described processes to occur at a hybrid interface, so that both up and down spin electrons initially diffuse from the organic into the surface, leaving the molecules in a vibronic excited state. The electrons in the surface can be then transferred back into the organic through the absorption of a number of vibrons. As the surface serves as a reservoir of angular momentum, the electrons transferred back to the organic do not necessarily have to conserve their spin. Together with the fact that the initial electron population on the molecule has a positive imbalance of majority electrons, this leads to an effective spin down "refilling" of the molecular state. For an electron-vibron coupling large enough this process lasts until a full spin depolarization of the electron population is achieved. This system evolution is enhanced via the described resonance mechanism. However, importantly, we found that the spin relaxation is present also when there is no exact resonance ($E_{\uparrow(\downarrow),0} \neq E_{\alpha,q}$ for all α and q), although it is slightly less pronounced. This is shown in Fig. 5, which displays the average number of electrons N_e, spin polarization S^z, and relative spin polarization S_P for $\tilde{\epsilon}_d = 3.5$. Furthermore, we note that the dependence of the results on $\tilde{\epsilon}_d$ indicates that, even if the spin relaxation is stronger for small $\tilde{\epsilon}_d$, it becomes important also for values a few times larger than $\hbar\omega$ for a large enough g. This is shown in Fig. 6, where the dependence of occupation probabilities $\{P_{\alpha,q}(t)\}$ on $\tilde{\epsilon}_d$ is plotted. For $\tilde{\epsilon}_d = 2$, the states $|\alpha, q = 0\rangle$ ($\alpha = \uparrow,\downarrow$) are in energy resonance with $|\alpha = 0, q = 2\rangle$ (i.e., $E_{\uparrow(\downarrow),0} = E_{0,2}$), and only $|\alpha = 0, q = 1\rangle$ is excited during the transient regime. Since the transitions from $|\alpha, q = 0\rangle$ ($\alpha = \uparrow,\downarrow$) to these two states have small associated FC matrix elements and, therefore, small rates already for $g = 2$, $|\alpha, q = 0\rangle$ ($\alpha = \uparrow,\downarrow$) are very long lived. Even more drastically, if we set $g = 4$, the refilling of $|\alpha = \downarrow, q = 0\rangle$ will be so fast that, after the initial decay, $P_{\downarrow,0}(t)$ inverts its trend and starts increasing until $P_{\downarrow,0}(t)$ becomes equal to $P_{\uparrow,0}(t)$ and the molecule is completely spin depolarized. In contrast, for $\tilde{\epsilon}_d = 6$, many states assume a nonzero probability during the transient time and the resonant

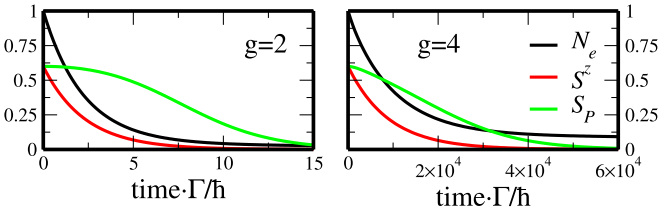

FIG. 5. (Color online) Time evolution of N_e, S^z, and S_P for $\tilde{\epsilon}_d = 3.5$ and $g = 2$ (left) and $g = 4$ (right) at $k_B T = 0.2$.

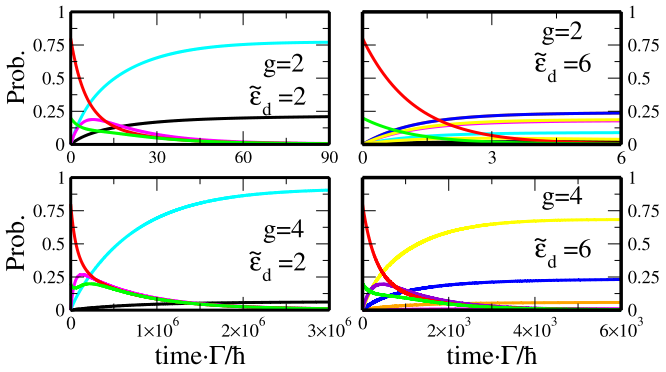

FIG. 6. (Color online) Time evolution of occupation probabilities $\{P_{\alpha,q}\}$ for $\tilde{\epsilon}_d = 2$ (left) and $\tilde{\epsilon}_d = 6$ (right) at $k_BT = 0.2$ and $\tilde{U} = 4$. Data are for $P_{0,0}$ (black lines), $P_{0,1}$ (cyan), $P_{0,2}$ (magenta), $P_{0,3}$ (orange), $P_{0,4}$ (blue), $P_{0,5}$ (yellow), $P_{0,6}$ (violet), $P_{\uparrow,0}$ (red), and $P_{\downarrow,0}$ (green).

state with $|\alpha,q=0\rangle$ ($\alpha = \uparrow,\downarrow$) is $|\alpha = 0,q = 6\rangle$. Now the refilling mechanism becomes important only for $g = 4$, when the FC matrix elements connecting the states with $q = 0$ and $q = 6$ are non-negligible.

Finally, we discuss the temperature dependence of the spin relaxation. Specifically, we note that increasing the temperature k_BT leads to a faster decay of both S^z and S_P. In fact, besides the resonant state, there are several other states with a large number of vibrons, which are progressively populated during the transient regime because of thermal smearing, and all of these relax in such a way to depolarize the molecule. This is shown in Fig. 7 (left panels), where we plot the time-dependent probabilities $\{P^{\alpha q}(t)\}$ at different temperatures $k_BT = 0.6$ and 1.4 and for $g = 3$, $\tilde{\epsilon}_d = 4$, and $\tilde{U} = 4$. The refilling of the state $|\alpha = \downarrow,q = 0\rangle$ is clearly visible for every temperature. However, now, alike for the case for $k_BT = 0.2$, the dynamics does not depend just on the energy resonance with the state $|\alpha = 0,q = 4\rangle$ and we observe that, during the transient phase, several states $|\alpha = 0,q \neq 0\rangle$ with higher energies than $E_{\alpha=\uparrow(\downarrow),q=0}$

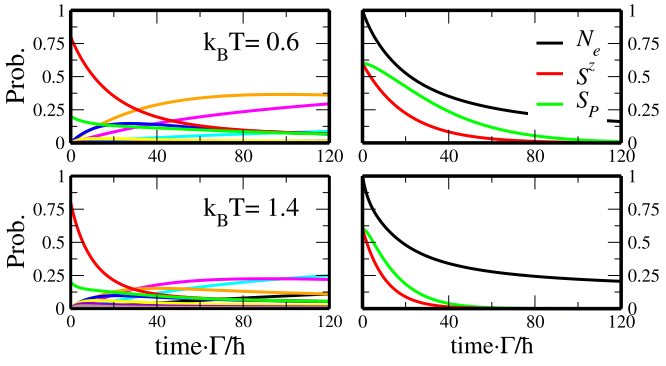

FIG. 7. (Color online) Time dependence of the occupation probabilities $\{P_{\alpha,q}\}$ (left panels) and of the average number of electrons N_e, spin polarization S^z, and relative spin polarization $S_P = S^z/N_e$ (right panels) for $k_BT = 0.6$ and 1.4 and $g = 3$. The renormalized on-site and charging energies are $\tilde{\epsilon}_d = 4$ and $\tilde{U} = 4$ like in Fig. 3. The results are for $P_{0,1}$ (cyan), $P_{0,2}$ (magenta), $P_{0,3}$ (orange), $P_{0,4}$ (blue), $P_{0,5}$ (yellow), $P_{0,6}$ (violet), $P_{\uparrow,0}$ (red), $P_{\downarrow,0}$ (green), and $P_{\uparrow\downarrow,0}$ (gray).

are progressively populated [for example, $P^{\alpha=0,q=5}(t)$ and $P^{\alpha=0,q=6}(t)$ for $k_BT = 1.4$]. However, those states can transit back to $|\alpha = \uparrow(\downarrow),q = 0\rangle$ at a large rate and, after an initial increase of their probabilities, they relax to the benefit of $P^{\alpha=\uparrow(\downarrow),q=0}$. This process dynamically re-establishes the equality between $P^{\alpha=\uparrow,q=0}$ and $P^{\alpha=\downarrow,q=0}$ so that, together with the energy-resonance mechanism, it leads to the decay of the spin-polarization S^z, which is shown in Fig. 7 (right panels). Besides, we note that, at the considered temperatures, the average occupation N_e does not go to zero even in the steady state as $|\alpha = \uparrow(\downarrow),q = 0\rangle$ has a finite probability.

IV. TRANSPORT AND EXPERIMENTAL IMPLICATIONS

We now turn our attention to discuss how the proposed spin-relaxation process can be addressed experimentally. Its main fingerprint is the crossover in the time evolution of the minority electron population from an initial fast exponential decay to a slower one, or, in some extreme cases, even to a slight enhancement, which lasts until the system is fully depolarized (see Fig. 3). In principle, one could look for evidence of such mechanism in the results of the recent 2PPE experiments of Steil *et al.* [27]. However, these experiments are, in practice, difficult to model quantitatively because of the amorphous nature of Co/Alq_3. In contrast, an alternative strategy consists in employing an experimental tool capable of probing single molecules and, therefore, here we propose the use of spSTM. In order to simulate a spSTM experiment, we connect the molecule to a ferromagnetic tip described through an additional spin-dependent coupling parameter $\Gamma_{\mathrm{tip},\sigma}$. Then, the constant $\Gamma_{s,\sigma}$ is replaced with $\Gamma_{\mathrm{tot},\sigma} = \Gamma_{s,\sigma} + \Gamma_{\mathrm{tip},\sigma}$ in the expression for the transition rates [Eq. (4)], and the time-dependent electrical current induced by the initial excitation of the molecule can be computed as

$$I(t) = -\frac{e}{\hbar}\sum_{\alpha,\alpha'}(n_{d,\alpha} - n_{d,\alpha'})R_{\alpha'q'\to\alpha q}\,P_{\alpha'q'}(t). \qquad (7)$$

The calculated time-dependent currents are shown in Fig. 8 for $\tilde{\epsilon}_d = 4$, $\tilde{U} = 4$, $k_BT = 0.2$, and for both $g = 0$ and $g = 4$. By switching the tip magnetization from parallel to antiparallel with respect to the molecule initial spin polarization [i.e., by inverting the ratio $\Gamma_{\mathrm{tip},\uparrow}/\Gamma_{\mathrm{tip},\downarrow}$ while keeping constant $P_{\uparrow,0}(0)/P_{\downarrow,0}(0)$], the time evolution of either the spin up or spin down electron population is probed (compare Figs. 3 and 8). Then, for large enough electron-vibron coupling ($g = 4$) and for tip/molecule parallel spin polarization, the refilling of the minority spin channel is seen as a transient regime that extends

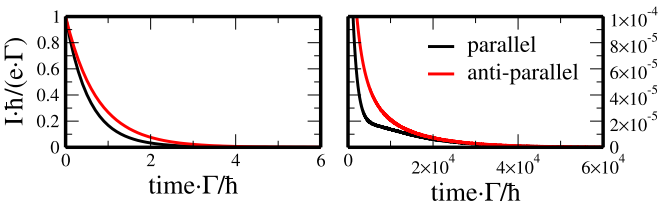

FIG. 8. (Color online) Time evolution of the current for the spSTM model with $g = 0$ (left panel) and $g = 4$ (right panel). Here $\tilde{\epsilon}_d = 4$, $k_BT = 0.2$, while $\Gamma_{\mathrm{tip},\downarrow} = 0.2\Gamma_{\mathrm{tip},\uparrow} = 0.2\Gamma$ (parallel) and $\Gamma_{\mathrm{tip},\uparrow} = 0.2\Gamma_{\mathrm{tip},\downarrow} = 0.2\Gamma$ (antiparallel) with, as before, $\Gamma = \Gamma_{s,\uparrow} = \Gamma_{s,\downarrow}$.

over a time-interval $\Delta t = \text{time} \cdot \Gamma/\hbar \approx 10^4$, during which the current decays slowly. Therefore, the value of Δt sets an upper bound to the time resolution that a spSTM experiment needs in order to be able to access the spin-relaxation dynamics. Notably, by assuming $\Gamma = 1$ meV (a realistic value for a molecule physisorbed on a surface) we can estimate Δt to be 26 ns for $g = 4$ and about an order of magnitude smaller if $g = 3$, with a current of the order of 1 nA. Since nanosecond resolution has been recently achieved in pump-probe spSTM experiments [29–32], a verification of our proposed vibron-induced spin relaxation at hybrid interfaces is possible.

V. CONCLUSIONS

In conclusion we have demonstrated that a spin-polarized electron population at a hybrid interface can undergo spin relaxation even in the absence of spin-orbit and hyperfine interaction. Our proposed mechanism is based on an electron exchange processes between the surface and the molecule, which is promoted by the electron-vibron coupling. We propose that this mechanism can be experimentally accessed using spSTM experiments.

ACKNOWLEDGMENTS

A.D. thanks Dr. Aitor Mugarza for an inspiring question, which stimulated some ideas about the STM simulations. This work is partly sponsored by the European Research Council, QUEST project. A.D. and I.R. thank the EU projects HINTS (NMP3-SL-2011-263104) and ACMOL (FP7-FET GA618082) for financial support.

[1] V. Dediu, L. E. Hueso, I. Bergenti, and C. Taliani, Nat. Mater. **8**, 707 (2009).
[2] S. Sanvito, Chem. Soc. Rev. **40**, 3336 (2011).
[3] S. Pramanik *et al.*, Nat. Nanotech. **2**, 216 (2007).
[4] G. Szulczewski, S. Sanvito, and M. Coey, Nat. Mater. **8**, 693 (2009).
[5] S. Bandyopadhyay, Phys. Rev. B **81**, 153202 (2010).
[6] C. Boehme and J. M. Lupton, Nat. Nanotech. **8**, 612 (2013).
[7] N. J. Harmon and M. E. Flatté, Phys. Rev. Lett. **110**, 176602 (2013).
[8] P. A. Bobbert, W. Wagemans, F. W. A. van Oost, B. Koopmans, and M. Wohlgenannt, Phys. Rev. Lett. **102**, 156604 (2009).
[9] J. J. H. M. Schoonus, P. G. E. Lumens, W. Wagemans, J. T. Kohlhepp, P. A. Bobbert, H. J. M. Swagten, and B. Koopmans, Phys. Rev. Lett. **103**, 146601 (2009).
[10] T. D. Nguyen *et al.*, Nat. Mater. **9**, 345 (2010).
[11] N. J. Rolfe, M. Heeney, P. B. Wyatt, A. J. Drew, T. Kreouzis, and W. P. Gillin, Phys. Rev. B **80**, 241201(R) (2009).
[12] Z. G. Yu, Phys. Rev. Lett. **106**, 106602 (2011); Phys. Rev. B **85**, 115201 (2012).
[13] L. Nuccio *et al.*, Phys. Rev. Lett. **110**, 216602 (2013).
[14] S. Watanabe *et al.*, Nat. Phys. **10**, 308 (2014).
[15] C. Barraud *et al.*, Nat. Phys. **6**, 615 (2010).
[16] S. Sanvito, Nat. Phys. **6**, 562 (2010).
[17] Y. Q. Zhan, I. Bergenti, L. E. Hueso, V. Dediu, M. P. de Jong, and Z. S. Li, Phys. Rev. B **76**, 045406 (2007).
[18] Y. Q. Zhan, M. P. de Jong, F. H. Li, V. Dediu, M. Fahlman, and W. R. Salaneck, Phys. Rev. B **78**, 045208 (2008).
[19] S. Shi *et al.*, Adv. Funct. Mater. **24**, 4812 (2014).
[20] A. Droghetti *et al.*, Phys. Rev. B **89**, 094412 (2014).
[21] S. Müller *et al.*, New. J. Phys. **15**, 113054 (2013).
[22] J. Brede, N. Atodiresei, S. Kuck, P. Lazić, V. Caciuc, Y. Morikawa, G. Hoffmann, S. Blügel, and R. Wiesendanger, Phys. Rev. Lett. **105**, 047204 (2010).
[23] N. Atodiresei, J. Brede, P. Lazić, V. Caciuc, G. Hoffmann, R. Wiesendanger, and S. Blügel, Phys. Rev. Lett. **105**, 066601 (2010).
[24] T. Methfessel, S. Steil, N. Baadji, N. Grossmann, K. Koffler, S. Sanvito, M. Aeschlimann, M. Cinchetti, and H. J. Elmers, Phys. Rev. B **84**, 224403 (2011).
[25] S. Lach *et al.*, Adv. Funct. Mater. **22**, 989 (2012).
[26] F. Djeghloul *et al.*, Sci. Rep. **3**, 1272 (2013).
[27] S. Steil *et al.*, Nat. Phys. **9**, 242 (2013).
[28] M. Pickel, A. B. Schmidt, F. Giesen, J. Braun, J. Minár, H. Ebert, M. Donath, and M. Weinelt, Phys. Rev. Lett. **101**, 066402 (2008).
[29] C. Grosse *et al.*, Appl. Phys. Lett. **103**, 183108 (2013).
[30] S. Loth *et al.*, Science **329**, 1628 (2010).
[31] S. Yan *et al.*, Nat. Nanotech. **10**, 40 (2015).
[32] S. Yoshida *et al.*, Nat. Nanotech. **9**, 588 (2014).
[33] T. Ohto, I. Rungger, K. Yamashita, H. Nakamura, and S. Sanvito, Phys. Rev. B **87**, 205439 (2013).
[34] N. S. Wingreen, K. W. Jacobsen, and J. W. Wilkins, Phys. Rev. Lett. **61**, 1396 (1988).
[35] A. Mitra, I. Aleiner, and A. J. Millis, Phys. Rev. B **69**, 245302 (2004).
[36] J. Koch and F. von Oppen, Phys. Rev. Lett. **94**, 206804 (2005).
[37] J. Koch, F. von Oppen, and A. V. Andreev, Phys. Rev. B **74**, 205438 (2006).
[38] A. Donabidowicz-Kolkowska and C. Timm, New J. Phys. **14**, 103050 (2012).
[39] I. G. Lang and Y. A. Firsov, Sov. Phys. JETP **16**, 1301 (1963).
[40] D. A. Ryndyk, R. Gutiérrez, B. Song, and G. Cuniberti, in *Energy Transfer Dynamics in Biomaterial Systems*, Springer Series in Chemical Physics Vol. 93 (Springer-Verlag, Berlin, 2009), pp. 213–335.
[41] The eigenstates $|\alpha,q\rangle$ of the Hamiltonian Eq. (1) are one-to-one equivalent to the eigenstates of the Hamiltonian obtained by the Lang-Firsov canonical transformation and they have the same eigenvalues [Eq. (2)] and quantum numbers α and q [40].
[42] H.-P. Breuer and F. Petruccione, *The Theory of Open Quantum Systems* (Oxford University Press, Oxford, UK, 2002).
[43] D. Gatteschi, R. Sessoli, and J. Villain, *Molecular Nanomagnets* (Oxford University Press, Oxford, UK, 2006).
[44] M. Cinchetti *et al.*, Nat. Mater. **8**, 115 (2009).
[45] We note that with our "collinear" choice for the initial conditions the diagonal and off-diagonal components of the density matrix are decoupled [38].
[46] E. Burzuri *et al.*, Nano Lett. **14**, 3191 (2014).